

Y-Aromaticity: Why Is the Trimethylenemethane Dication More Stable than the Butadienyl Dication?

Amy Dworkin, Rachel Naumann, Christopher Seigfred, and Joel M. Karty*

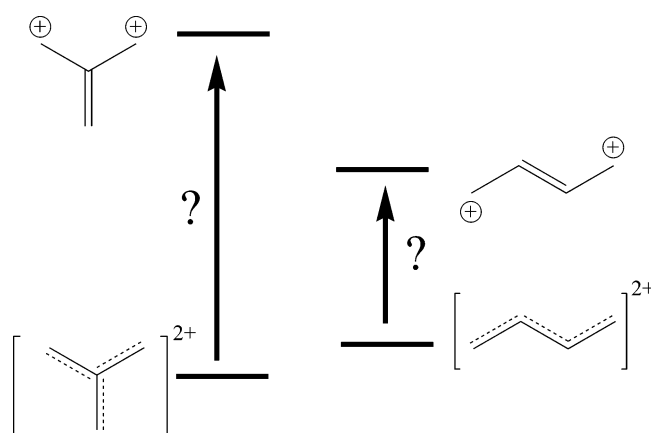
Department of Chemistry, Elon University, 2625 Campus Box, Elon, North Carolina 27244

Yirong Mo*

Department of Chemistry, Western Michigan University, Kalamazoo, Michigan 49008-3842

jkarty@elon.edu; yirong.mo@wmich.edu

Received April 21, 2005



Resonance energies of the trimethylenemethane dication (**1**) and the butadienyl dication (**4**) were evaluated using two independent computational methodologies to provide insight into the validity of Y-aromaticity. One methodology employed density functional theory calculations and examined the resonance contribution of the C=C double bond toward the double hydride abstraction enthalpies of methylpropene (**6**) and 2-butene (**8**), yielding **1** and **4**, respectively. These resonance contributions by the double bond were determined by calculating the double hydride abstraction enthalpies of both the parallel and perpendicular conformations of vinylogues of **6** and **8**, in which $n = 1-4$ vinyl units were inserted between the central carbon-carbon double bond and each of the reaction centers. Extrapolation of the resonance contribution in each vinylogue to $n = 0$ yielded the resonance contribution in the respective parent molecules. The second methodology employed an orbital deletion procedure (ODP), which effectively allowed us to examine the energies of individual resonance structures. The resonance energy of each dication is computed as the difference between the most stable resonance structure and that of the delocalized species. The two methodologies are in agreement, suggesting that the resonance energy of the trimethylenemethane dication is substantially greater than that of the butadienyl dication. The origin of this difference in resonance stabilization is discussed.

Introduction

Y-aromaticity has been the subject of much debate for over 30 years.¹⁻¹⁶ Aromaticity, in the conventional sense, arises when Hückel's number (i.e., $4n + 2$) of π -electrons occupy a completely conjugated ring system. Y-aroma-

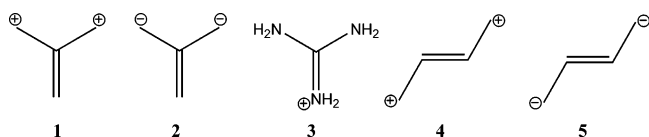
ticity is an extension of this definition, suggesting that aromaticity need not rely on conjugation around a ring but may also take place through a central atom (so-called cross-conjugation).⁴ The trimethylenemethane dication (**1**, TMM²⁺) and dianion (**2**, TMM²⁻), which possess 2 and 6 π -electrons, respectively, are archetypal Y-aromatic species.

Klein and Medlik¹⁻³ invoked arguments of Y-aromaticity to support the facile formation of the trimethylen-

(1) Klein, J.; Medlik, A. *J. Chem. Soc., Chem. Commun.* **1973**, 275.
 (2) Bates, W. A.; Beaven, W. A.; Greene, M. G.; Klein, J. H. *J. Am. Chem. Soc.* **1974**, *96*, 5640.

emethane dianion (**2**, TMM^{2-}) in solution. Gund⁴ suggested that Y-aromaticity is the reason for the unusual stability of the guanidinium ion (**3**) in boiling water. Indeed, simple Hückel molecular orbital (MO) theory predicts greater resonance energy for the Y-shaped ions, TMM^{2+} and TMM^{2-} , than for their linear counterparts, **4** and **5**, respectively.^{5,6} In support of this, Agranat and Skancke, upon examination of calculated barriers for the simultaneous rotation of **1**, **2**, and **3** methylene groups in TMM^{2-} , concluded that TMM^{2-} is unequivocally “distinguished by a novel enhanced stabilization and charge alternation”.⁷ Krygowski and co-workers,⁸ in their computational study on the guanidinium ion and its derivatives, claim that the guanidinium ion is reminiscent of benzene in its resistance to perturbations in π -electron delocalization. NMR studies have also provided support for Y-aromaticity. Mills and co-workers⁹ showed that the correlation between the ¹H NMR chemical shift and the π -electron density of TMM^{2-} is consistent with observations of traditional aromatic species. Rajca and Tolbert¹⁰ used ¹³C NMR to evaluate the aromaticity of substituted methylenemethane dianions.

A number of computational studies, however, have cast doubt on the validity of Y-aromaticity. Radhakrishnan and Agranat¹¹ noted that TMM^{2+} is not much more stable than its linear analogue, the butadienyl dication (**4**, BD^{2+}), and they further showed that the reverse is true in more extensively conjugated systems. Moreover, Agranat and co-workers¹² showed that the inclusion of diffuse orbitals and electron correlation in their calculations, in fact, places TMM^{2-} at a higher energy than its linear analogue, the butadienyl dianion (**5**, BD^{2-}). This was confirmed by Skancke,¹³ who showed that at the G2 level of theory BD^{2-} is more stable than TMM^{2-} by 39.3 kcal/mol. Sommerfeld¹⁴ performed a novel study on TMM^{2-} and BD^{2-} in which he calculated the electron autodetachment lifetimes of these unstable dianions in the gas phase. Although he found that the lifetime of TMM^{2-} is slightly longer than that of BD^{2-} , there was no conclusive evidence supporting Y-aromaticity in TMM^{2-} .



Along with discrediting the notion of Y-aromaticity, computational studies have also offered explanations as to why TMM^{2-} and **3** appear to exhibit unusual stability

in solution. Wiberg¹⁵ has suggested that the stability of TMM^{2-} arises from favorable Coulombic attraction with the lithium cations in solution. The stability of **3**, on the other hand, is likely a result of hydrogen bonding with the solvent.¹⁶ Skancke,¹³ in fact, showed that **3** is stabilized intrinsically by a network of intramolecular hydrogen bonds.

A critical piece of information that is noticeably absent from the debate over Y-aromaticity is an evaluation of the resonance energy of a cross-conjugated species, especially in comparison to its linear analogue. The reason these values are important is that much of the recent focus arguing against the notion of Y-aromaticity has been on the overall stabilities of the Y- vs the linear-shaped species. However, these relative *overall* stabilities, contributed by both the σ - and π -components, do *not* provide accurate representations of relative resonance stabilization resulting from π -electron delocalization only. As we demonstrate throughout the rest of this paper, nonresonance effects (inductive effects and field effects (charge repulsion)) can also play a significant role in those energy differences.

In fact, the importance of the inductive and field effects should not be surprising. The different topologies of the Y-shaped ions allow for different distributions of charge, affecting both charge location and charge concentration. These two factors may be expected to have a profound effect on the internal charge repulsion. Moreover, it is well-known that sp^2 hybridization invokes electron-withdrawing character on nearby atoms.¹⁷ Indeed, we have shown in a previous study¹⁸ that these inductive effects destabilize the allyl cation relative to the propyl cation and stabilize the allyl anion relative to the propyl anion. Because of different topologies (Y-shaped vs linear), those electron-withdrawing atoms are arranged differently with respect to nearby charges. Consequently, the inductive effects provided by the presence of the formal double bond are not expected to be the same for both topologies.

Here, we have evaluated the effects from both the resonance and the nonresonance (inductive/field) effects on the stability of TMM^{2+} and BD^{2+} . We chose to study the dications primarily to avoid complications with the pyramidal geometries in the dianions.¹⁶ We employed two different computational methodologies. One is an extrapolative methodology using density functional theory (DFT) calculations, which we developed and have applied to other systems.^{18,19} The second is an orbital deletion procedure (ODP) technique, which can compute the adiabatic resonance energy on the basis of the conventional Pauling–Wheland definition.²⁰ From these two methodologies, we have found that the resonance energy of TMM^{2+} is roughly 2–3 times that of BD^{2+} . Compensating for this, it appears that the inductive/field effects

(3) Klein, J.; Medlik-Balan, A.; Meyer, A. Y.; Chorev, M. *Tetrahedron* **1976**, *32*.

(4) Gund, P. *J. Chem. Educ.* **1972**, *49*, 100.

(5) Finnegan, R. A. *Ann. N. Y. Acad. Sci.* **1969**, *159*, 242–266.

(6) Note: we have repeated the Hückel calculations here and arrived at 0.228 β greater resonance stabilization in both Y-shaped ions.

(7) Agranat, I.; Skancke, A. *J. Am. Chem. Soc.* **1985**, *107*, 867.

(8) Krygowski, T. M.; Cyranski, M. K.; Anulewics-Ostrowska, R. *Pol. J. Chem.* **2001**, *75*, 1939–1942.

(9) Mills, N. S.; Shapiro, J.; Hollingsworth, M. *J. Am. Chem. Soc.* **1981**, *103*, 1263.

(10) Rajca, A.; Tolbert, L. M. *J. Am. Chem. Soc.* **1985**, *107*, 698–699.

(11) Radhakrishnan, T. P.; Agranat, I. *J. Org. Chem.* **2001**, *66*, 3215.

(12) Agranat, I.; Radhakrishnan, T. P.; Herndon, W. C.; Skancke, A. *Chem. Phys. Lett.* **1991**, *181*, 117.

(13) Skancke, A. *J. Phys. Chem.* **1994**, *98*, 5234–5239.

(14) Sommerfeld, T. *J. Am. Chem. Soc.* **2002**, *124*, 1119–1124.

(15) Wiberg, K. B. *J. Am. Chem. Soc.* **1990**, *112*, 4177.

(16) Gobbi, A.; Frenking, G. *J. Am. Chem. Soc.* **1993**, *115*, 2362–2372.

(17) Lowry, T. H.; Richardson, K. S. *Mechanism and Theory in Organic Chemistry*, 3rd ed.; HarperCollins: New York, 1987.

(18) Barbour, J. B.; Karty, J. M. *J. Org. Chem.* **2004**, *69*, 648.

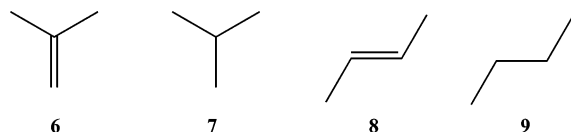
(19) Holt, J.; Karty, J. M. *J. Am. Chem. Soc.* **2003**, *125*, 2797.

(20) Wheland, G. W. *The Theory of Resonance*; John Wiley & Sons: New York, 1944.

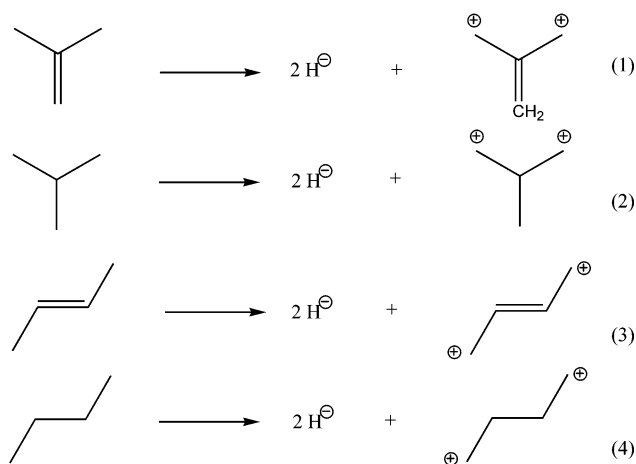
serve to destabilize both dications but that destabilization is more pronounced for BD^{2+} .

Methodologies

Vinylogue Methodology. To study the resonance and the inductive/field effects on the stabilities of TMM^{2+} and BD^{2+} , we chose to examine the double hydride abstraction reactions of 2-methylpropene (**6**) and 2-butene (**8**) (eqs 1 and 3, respectively), in which the ions of interest are products. We also examined the double hydride abstraction of 2-methylpropane (**7**) and butane (**9**) (eqs 2 and 4, respectively), which will be referred to as the respective reference compounds to **6** and **8**. In **7** and **9**, there is no



central π -bond that can participate in resonance. In addition, the sp^3 hybridization of the two central carbon atoms in **7** and **9** is taken to be neither electron withdrawing nor significantly electron donating.



To determine the resonance and the field/inductive contributions to the reactions in eqs 1 and 3, we calculated the double hydride abstraction enthalpies of several vinylogues of **6** and **8**, in which $n = 1-4$ vinyl units were inserted between each reaction center (i.e., CH_3) and the rest of the molecule (Figure 1). The geometry-optimized structures of the vinylogues are those in which all carbon atoms are coplanar and are hereafter referred to as the parallel conformations. We also calculated the double hydride abstraction enthalpies of those vinylogues in which the central double bond was constrained to be perpendicular to the two conjugated chains. In these perpendicular conformations, the central double bond was isolated from the reaction centers with respect to resonance.¹⁷ Finally, we calculated the double hydride abstraction enthalpies of the vinylogues of **7** and **9**. Just as in the parent molecules, no resonance or inductive/field effect contributions were provided by the central C–C single bond in these reference vinylogues because of the sp^3 hybridization.

For each parallel vinylogue of **6** and **8**, the resonance contribution toward the double hydride abstraction en-

thalpy was computed as the difference in the reaction enthalpy between the parallel and perpendicular conformations. The inductive/field contributions, on the other hand, were computed as the difference in the reaction enthalpy between the perpendicular vinylogue and the reference vinylogue. The resonance contributions were then plotted for each n and extrapolated back to $n = 0$ (the parent compound). Similarly, the inductive/field contributions were plotted and extrapolated back to $n = 0$.

This methodology is validated, in large part, by the agreement between the independent extrapolations of the resonance and inductive/field contributions. At $n = 0$, the resonance and inductive/field contributions should add up to the difference in the double hydride abstraction enthalpies between the compound of interest and the reference compound (i.e., the difference in reaction enthalpy between **6** and **7** for the Y-topology and the difference in reaction enthalpy between **8** and **9** for the linear topology).

As additional validation, we have shown in a previous paper²¹ that a similar extrapolative methodology was in excellent agreement with results from linear free energy relationships. In that study, we evaluated the resonance and inductive contributions toward the acidity of several para-substituted phenols, spanning a range in gas-phase acidity of about 27 kcal/mol. Furthermore, our results in previous studies using this vinylogue methodology have been in good qualitative agreement with computational approaches using valence bond (and related) calculations.^{22,23}

Orbital Deletion Procedure (ODP) Methodology. The ODP procedure we employed²⁴⁻²⁹ allowed us to study electron delocalization in the two parent dications **1** and **4** by removing the vacant π -orbitals from the expansion space of molecular orbitals on the cationic carbons. This ODP method is applicable to carbocations and boranes and can further be extended to the block-localized wave function (BLW) method which uniquely combines the advantages of both the molecular orbital and valence bond theories.³⁰⁻³⁷

(21) Barbour, J. B.; Karty, J. M. *J. Phys. Org. Chem.* **2005**, *18*, 210–216.

(22) Hiberty, P. C.; Byrman, C. P. *J. Am. Chem. Soc.* **1995**, *117*, 9875–9880.

(23) Mo, Y.; Zhenyang, L.; Wu, W.; Zhang, Q. *J. Phys. Chem.* **1996**, *100*, 6469.

(24) Mo, Y.; Lin, Z. *J. Chem. Phys.* **1996**, *105*, 1046–1051.

(25) Mo, Y.; Schleyer, P. v. R.; Jiao, H.; Lin, Z. *Chem. Phys. Lett.* **1997**, *280*, 439–443.

(26) Mo, Y.; Jiao, H.; Lin, Z.; Schleyer, P. v. R. *Chem. Phys. Lett.* **1998**, *289*, 383–390.

(27) Mo, Y.; M., L.; Wu, W.; Zhang, Q.; Schleyer, P. v. R. *Sci. China, Ser. B* **1999**, *42*, 253–260.

(28) Mo, Y.; Wu, W.; Zhang, Q. *J. Chem. Phys.* **2003**, *119*, 6448–6456.

(29) Mo, Y.; Jiao, H.; Schleyer, P. v. R. *J. Org. Chem.* **2004**, *69*, 3493–3499.

(30) Mo, Y.; Peyerimhoff, S. D. *J. Chem. Phys.* **1998**, *109*, 1687.

(31) Mo, Y.; Zhang, Y.; Gao, J. *J. Am. Chem. Soc.* **1999**, *121*, 5737–5742.

(32) Mo, Y.; Gao, J.; Peyerimhoff, S. D. *J. Chem. Phys.* **2000**, *112*, 5530–5538.

(33) Mo, Y.; Subramanian, G.; Ferguson, D. M.; Gao, J. *J. Am. Chem. Soc.* **2002**, *124*.

(34) Mo, Y.; Song, L.; Wu, W.; Zhang, Q. *J. Am. Chem. Soc.* **2004**, *126*, 3974–3982.

(35) Mo, Y. *J. Org. Chem.* **2004**, *69*, 5563–5567.

(36) Mo, Y.; Gao, J. *J. Phys. Chem. A* **2000**, *104*, 3012–3020.

(37) Mo, Y.; Gao, J. *J. Comput. Chem.* **2000**, *21*, 1458–1469.

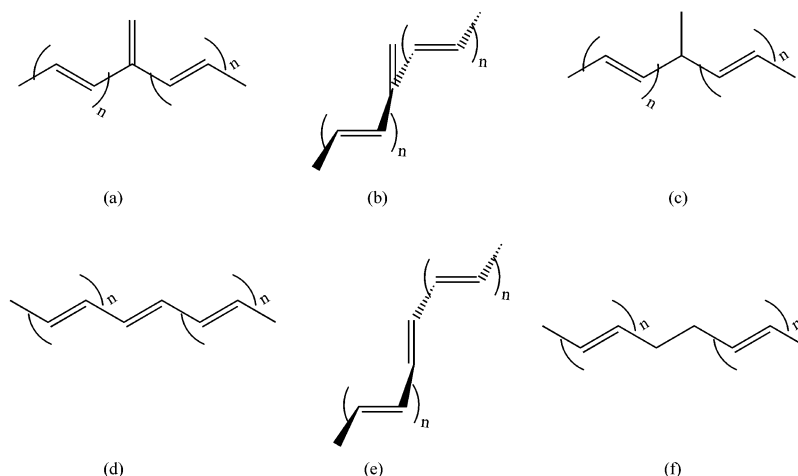


FIGURE 1. (a) Parallel vinylogue of **6**. (b) Perpendicular vinylogue of **6**. (c) Vinylogue of **7**. (d) Parallel vinylogue of **8**. (e) Perpendicular vinylogue of **8**. (f) Vinylogue of **9**.

For carbocations, the electronic interaction comes from the vicinal occupied fragmental molecular orbitals and the vacant p_{π} -orbitals on the cationic carbon. Thus, carbocations can be well studied by removing the p_{π} -orbitals from the orbital expansion space to derive the wave function Ψ^{Loc} for the reference state, i.e., the most stable resonance structure. Because normal molecular orbital calculations lead to a wave function, Ψ^{Del} , which corresponds to a delocalized state and is a combination of all possible resonance structures, the magnitude of the resonance is determined by the energy change resulting from the removal of p_{π} -orbitals. That is,

$$\Delta E_{\text{re}} = E(\Psi^{\text{Loc}}) - E(\Psi^{\text{Del}}) \quad (5)$$

It should be emphasized here that both Ψ^{Loc} and Ψ^{Del} are optimized *self-consistently*, and the ODP approach is *not* a post-SCF technique. This enables us to perform geometrical optimizations with the electron delocalization quenched. In addition, eq 5 follows the definition of resonance energy by Pauling and Wheland, as the resonance energy is “obtained by subtracting the actual energy of the molecule in question from that of the most stable contributing structure”.²⁰

We computed two types of resonance energy, which depended on the geometries employed. The vertical resonance energy (VRE) is the energy difference between the geometry-optimized ground state and its most stable resonance contributor at the same geometry, whereas the adiabatic resonance energy (ARE) is the energy difference between the geometry-optimized ground state and the geometry-optimized resonance structure; i.e., both geometries are relaxed. The difference between the VRE and the ARE reflects the compression energy for the σ -frame.

We should note that our vinylogue methodology should reflect the AREs more than the VREs. This is because in the vinylogue methodology we perform geometry optimizations on the perpendicular vinylogues, allowing the angles and bond lengths to relax.

Computational Details

Vinylogue Methodology. All enthalpies reported were calculated using the Gaussian 98W software package.³⁸ Geometries were optimized with density functional theory (DFT) at the B3LYP level of theory³⁹ using the 6-31+G* basis set. This is the same level of theory and basis set as was used in our previous vinylogue studies,^{19,40} which have proven to be in excellent agreement with available experimental reaction thermodynamics, as well as with other resonance studies. Furthermore, the enthalpy *differences* we calculated at that level of theory are in excellent agreement with those obtained at the G2 level of theory (see Results and ref 19).

Frequency calculations were performed to obtain enthalpies thermally corrected to 298 K and to ensure that each geometry was a true energy minimum. All frequencies were real. Input geometries for Gaussian were obtained from AM1 optimized geometries using PC Spartan Pro.

All double bonds in the conjugated chains of the vinylogues were constructed in the E conformation. Furthermore, in each perpendicular vinylogue, the two conjugated chains were rotated in opposite directions with respect to the central C=C double bond, giving them an overall C_2 symmetry (Figure 1b,e). Although we did not make certain that these were global energy minimized structures for the vinylogues, such geometric constraints are critical for two reasons: (1) they ensure that errors resulting from steric and charge repulsion from the two conjugated chains are kept to a minimum, and (2) they ensure that any errors that are introduced in calculating the absolute double hydride abstraction enthalpies will largely be cancelled in taking *differences* in reaction enthalpies.

Orbital Deletion Procedure Methodology. The ODP method, which is a special case of the BLW method,^{30,32} can be realized conveniently by slightly modifying any existing

(38) Frisch, M. J.; Trucks, G. W.; Schlegel, H. B.; Scuseria, G. E.; Robb, M. A.; Cheeseman, J. R.; Zakrzewski, V. G.; Montgomery, J. A., Jr.; Stratmann, R. E.; Burant, J. C.; Dapprich, S.; Millam, J. M.; Daniels, A. D.; Kudin, K. N.; Strain, M. C.; Farkas, O.; Tomasi, J.; Barone, V.; Cossi, M.; Cammi, R.; Mennucci, B.; Pomelli, C.; Adamo, C.; Clifford, S.; Ochterski, J.; Petersson, G. A.; Ayala, P. Y.; Cui, Q.; Morokuma, K.; Malick, D. K.; Rabuck, A. D.; Raghavachari, K.; Foresman, J. B.; Cioslowski, J.; Ortiz, J. V.; Stefanov, B. B.; Liu, G.; Liashenko, A.; Piskorz, P.; Komaromi, I.; Gomperts, R.; Martin, R. L.; Fox, D. J.; Keith, T.; Al-Laham, M. A.; Peng, C. Y.; Nanayakkara, A.; Gonzalez, C.; Challacombe, M.; Gill, P. M. W.; Johnson, B. G.; Chen, W.; Wong, M. W.; Andres, J. L.; Head-Gordon, M.; Replogle, E. S.; Pople, J. A. *Gaussian 98*, Gaussian, Inc.: Pittsburgh, PA, 1998.

(39) (a) Becke, A. D. *J. Chem. Phys.*, **98**, 5648–5652. (b) Lee, C.; Yang, W.; Parr, R. G. *Phys. Rev. B* **1988**, *37*, 785–789. Miehlich, B.; Savin, A.; Stoll, H.; Preuss, H. *Chem. Phys. Lett.* **1989**, *157*, 200–206.

(40) Barbour, J. B.; Karty, J. M. *J. Phys. Org. Chem.*, in press.

TABLE 1. DFT-Calculated (B3LYP/6-31+G*) Double Hydride Abstraction Enthalpies ($\Delta_{\text{DHA}}H^0$) of Y-Shaped Vinylogues

n	$\Delta_{\text{DHA}}H^0$ (parallel) (kcal/mol)	$\Delta_{\text{DHA}}H^0$ (perpendicular) (kcal/mol)	$\Delta_{\text{DHA}}H^0$ (reference) (kcal/mol)	DFT resonance contribution ^a (kcal/mol)	Hückel resonance energy (β)	DFT inductive contribution ^b (kcal/mol)	$1/(n+1)$
0	731.6		745.7		1.464		1
1	630.6	646.3	635.2	15.7	1.172	-11.1	0.500
2	577.3	585.5	578.3	8.1	1.100	-7.2	0.333
3	542.3	548.1	543.1	5.8	1.074	-5.0	0.250
4	518.1	522.9	519.0	4.8	1.056	-3.9	0.200

^a $\Delta_{\text{DHA}}H^0$ (perpendicular) - $\Delta_{\text{DHA}}H^0$ (parallel). ^b $\Delta_{\text{DHA}}H^0$ (reference) - $\Delta_{\text{DHA}}H^0$ (perpendicular).

TABLE 2. DFT-Calculated (B3LYP/6-31+G*) Double Hydride Abstraction Enthalpies ($\Delta_{\text{DHA}}H^0$) of Linear Vinylogues

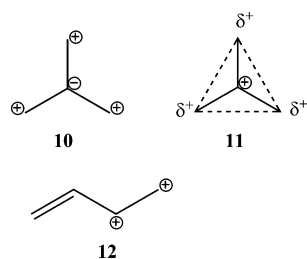
n	$\Delta_{\text{DHA}}H^0$ (parallel) (kcal/mol)	$\Delta_{\text{DHA}}H^0$ (perpendicular) (kcal/mol)	$\Delta_{\text{DHA}}H^0$ (reference) (kcal/mol)	DFT resonance contribution ^a (kcal/mol)	Hückel resonance energy (β)	DFT inductive contribution ^b (kcal/mol)	$1/(n+1)$
0	739.4		723.7		0.828		1
1	626.9	634.7	618.8	7.8	0.398	-15.9	0.500
2	571.4	576.7	567.1	5.3	0.264	-9.6	0.333
3	537.3	541.5	534.5	4.2	0.198	-7.0	0.250
4	513.9	517.5	512.4	3.6	0.156	-5.1	0.200

^a $\Delta_{\text{DHA}}H^0$ (perpendicular) - $\Delta_{\text{DHA}}H^0$ (parallel). ^b $\Delta_{\text{DHA}}H^0$ (reference) - $\Delta_{\text{DHA}}H^0$ (perpendicular).

quantum mechanical code, such as Gaussian 98.³⁸ Calculations were performed at the HF level, using both the 6-31G(d) and the 6-311+G(d,p) basis sets. To deactivate the selected basis functions, we assigned a high positive value (10^5 au) to their one-electron integrals and set their overlap integrals with the remaining basis functions to zero. Consequently, these basis functions were unable to accommodate significant electron density, and their corresponding populations as well as their contribution to the molecular wave function were essentially null. This ensures that the electronic effect we are examining, resonance, is effectively turned off.

We calculated the energies of resonance structures represented by **1** and **4**, which are predicted by simple resonance theory to be the most stable resonance structures of TMM^{2+} and BD^{2+} , respectively; the number of octets is maximized and internal charge repulsion is minimized. We were able to examine **1** by removing the orbital contribution from two of the three terminal carbon atoms in TMM^{2+} , and we were able to examine **4** by removing the orbital contribution of both terminal carbon atoms in BD^{2+} . Energies of **1** and **4** were calculated at both the geometry of the delocalized structure (i.e., the vertical geometry) and at the optimal geometry of the localized structure (i.e., the adiabatic geometry).

For comparison, we calculated the energies of two other unique resonance structures of TMM^{2+} , **10** and **11**, and of one other unique resonance structure of BD^{2+} , **12**. Calculations on **10** were accomplished by removing orbital contributions from all three terminal carbon atoms of TMM^{2+} , calculations on **11** were accomplished by removing orbital contributions from only the central carbon atom of TMM^{2+} , and calculations on **12** were accomplished by removing orbital contributions C1 and C2 of BD^{2+} . Other localized structures are possible but are predicted by simple resonance theory not to be the most stable.



Results

At the G2 level of theory, TMM^{2+} was calculated to be 9.1 kcal/mol more stable than BD^{2+} . At the B3LYP/6-31+G* level, that difference was calculated to be 8.8 kcal/mol.

Table 1 contains the DFT-calculated double hydride abstraction enthalpies of the parallel and perpendicular vinylogues of **6**, as well as of the vinylogues of the Y-shaped reference compound **7**. Table 1 also contains the resulting resonance and inductive/field effects of each Y-shaped vinylogue. Table 2 contains analogous DFT numbers for the linear species.

Figure 2 is a plot of the resonance contribution of the central C=C double bond toward the double hydride abstraction enthalpies of the Y-shaped vinylogues as a function of the Hückel resonance energies of the corresponding dications in units of β (see Discussion). Figure 3 is an analogous plot for the resonance contributions involving the linear vinylogues. Figures 4 and 5 are plots of the inductive/field contributions toward the double hydride abstraction enthalpies of the Y-shaped and linear vinylogues, respectively.

Table 3 contains the relative energies of **1** and **4** for our ODP study. These resonance structures are predicted by simple resonance theory and verified by the ODP calculations on other possible structures (Table 3) to be the most stable resonance structures of TMM^{2+} and BD^{2+} , respectively. Relative energies are calculated both at the optimized geometry of the delocalized structure (vertical geometry) and at the optimized geometry of the localized structure (adiabatic geometry). Table 3 also contains the relative energies of other resonance structures of TMM^{2+} and BD^{2+} . Table 4 contains structural parameters of **1** and **4**, and Table 5 contains both the vertical and the adiabatic resonance energies of each dication.

Discussion

A. Vinylogue Methodology. Our DFT calculations show that the double hydride abstraction of methylpropene (**6**) is less endothermic than that of 2-butene (**8**) by 7.8 kcal/mol (Tables 1 and 2). That difference is close

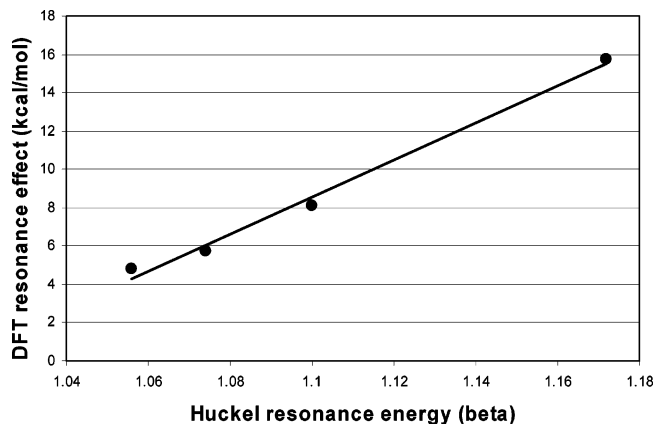


FIGURE 2. Resonance effects in the Y-shaped vinylogues plotted against the Hückel resonance energy of TMM^{2+} , in units of β .

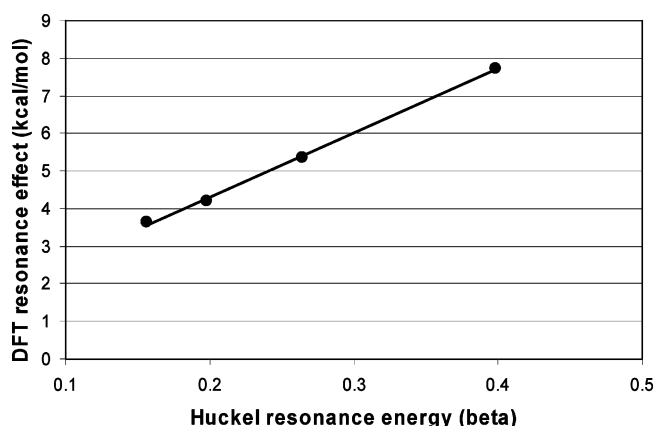


FIGURE 3. Resonance effects in the linear vinylogues plotted against the Hückel resonance energy of TMM^{2+} , in units of β .

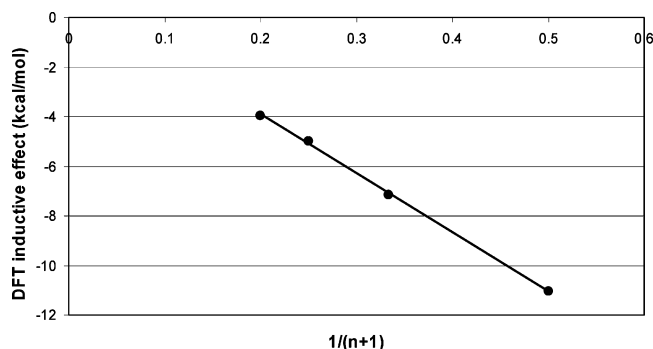


FIGURE 4. Inductive/field effects in the Y-shaped vinylogues plotted against $1/(n+1)$, where n is the number of inserted vinyl units.

to the 8.8 kcal/mol⁴¹ (B3LYP/6-31+G*) lower enthalpy of the TMM^{2+} dication over BD^{2+} . This strongly suggests that our study of the double hydride abstraction enthalpies ($\Delta_{\text{DHA}}H^0$) to provide insight into the origin of the difference in stability between the two dications is well founded.

(41) Radhakrishnan and Agranat (*J. Org. Chem.* **2001**, *66*, 3215) report the value to be between 8.2 and 9.2 kcal/mol using MP2, MP4, and B3LYP calculations.

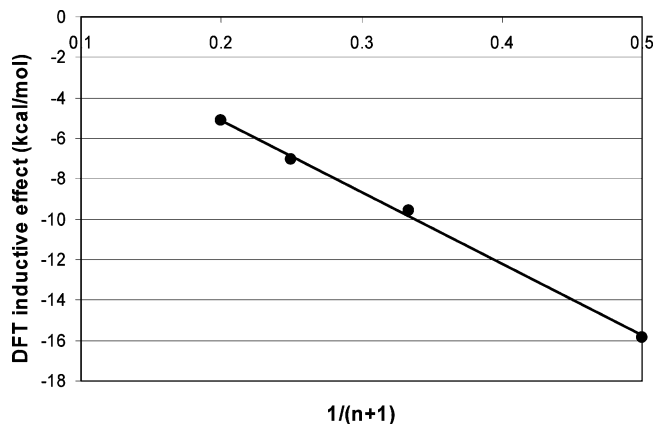


FIGURE 5. Inductive/field effects in the linear vinylogues plotted against $1/(n+1)$, where n is the number of inserted vinyl units.

As mentioned in the Introduction, we cannot simply take the 8.8 kcal/mol difference in stability between BD^{2+} and TMM^{2+} to be a measure of the difference in resonance energy, for two reasons: (1) The sp^2 -hybridized carbon atoms of the formal double bonds are electron withdrawing (Figure 6), which serves to destabilize the positive charges of the dications inductively. (2) The distribution of the +2 charge throughout each dication leads to charge repulsion, i.e., field effects. Because of the different topologies of TMM^{2+} (Y-shaped) and BD^{2+} (linear), the destabilization caused by each effect is expected to be different.

There are a number of noticeable trends in Tables 1 and 2. First, we see that for each set of vinylogues the double hydride abstraction enthalpy decreases with increasing n . Part of this is due to the additional resonance stabilization in the dication with each addition of a vinyl group. It is also, in part, due to the additional polarizability with increasing n . A more polarizable species is better able to stabilize a charge by internal solvation of that charge.⁴²

A second trend involves the comparison of the parallel and perpendicular vinylogues. Each parallel vinylogue has a lower double hydride abstraction enthalpy than the corresponding (same n) perpendicular vinylogue. We can conclude from this that the central double bond in each parallel vinylogue indeed serves to stabilize the dications via resonance.

A third trend shows that each perpendicular vinylogue has a *higher* double hydride abstraction enthalpy than the corresponding (same n) reference molecule. This confirms that the presence of the central $\text{C}=\text{C}$ double bond facilitates *destabilization* in the product dication via inductive/field effects. In Tables 1 and 2, this is manifest as negative values for the inductive effects.

A final trend shows that the magnitudes of both the resonance and inductive/field effects contributed by the central $\text{C}=\text{C}$ double bond decrease with increasing n . The diminishing inductive/field effects are explained by the increasing distance between the central $\text{C}=\text{C}$ double bond and the reaction centers and by the increasing delocalization of charge.

(42) Brauman, J. I.; Blair, L. K. *J. Am. Chem. Soc.* **1970**, *92*, 5986.

TABLE 3. Relative Energies^a (kcal/mol) of Delocalized and Localized Forms of TMM²⁺ and BD²⁺ Using the 6-311+G(d,p) (HF/6-31G(d)) Basis Set

structure ^b	TMM ²⁺		structure ^b	BD ²⁺	
	vertical geometry ^c	adiabatic geometry ^d		vertical geometry ^c	adiabatic geometry ^d
delocalized	0(0)		delocalized	16.7 (16.7)	
1	55.6 (56.3)	48.1 (48.9)	4	47.5 (48.3)	44.7 (45.4)
10	99.1 (100.5)	97.1 (99.2)	12	123.9 (126.6)	100.2 (102.6)
11	173.2 (178.3)	171 (177)			

^a All energies are relative to that of TMM²⁺. ^b Structures are described in the text. ^c The vertical geometry is the optimal geometry of the fully delocalized structure. ^d The adiabatic geometry is the optimal geometry of the localized resonance structure.

TABLE 4. Structural Parameters of the Delocalized (HF) Forms of TMM²⁺ and BD²⁺ Dications and of Their Geometry-Optimized Resonance Structures (ODP)

species	basis set	HF		ODP	
		R _{C-C} (Å)	R _{C=C} (Å)	R _{C-C} (Å)	R _{C=C} (Å)
TMM ²⁺	6-31G(d)	1.414	1.414	1.488	1.343
	6-311+G(d,p)	1.413	1.413	1.491	1.342
BD ²⁺	6-31G(d)	1.462	1.350	1.513	1.319
	6-311+G(d,p)	1.463	1.348	1.516	1.318

TABLE 5. Vertical Resonance Energy (VRE) and Adiabatic Resonance Energy (ARE) of TMM²⁺ and BD²⁺

species	basis set	VRE ^a	ARE ^b
TMM ²⁺	6-31G(d)	56.3	48.9
	6-311+G(d,p)	55.6	48.1
BD ²⁺	6-31G(d)	31.6	28.7
	6-311+G(d,p)	30.9	28.0

^a The vertical resonance energy (VRE) is the energy difference between the fully delocalized structure and the most stable resonance structure at the same geometry. ^b The adiabatic resonance energy (ARE) is the energy difference between the fully delocalized structure and the geometry optimized resonance structure.

**FIGURE 6.** Electron withdrawing character of the sp²-hybridized carbon atoms of the formal C=C double bonds as the source of inductive effects on the stability of (a) TMM²⁺ and (b) BD²⁺.

The decreasing resonance effect, on the other hand, can be explained using a simple “particle in a box” argument. The energy, $E(L)$, of a particle in a one-dimensional “box” is inversely proportional to the length of the box, L . Therefore, a change in L for a “box” of a given length will have a greater effect on $E(L)$ than the same change in L for a longer “box”.

A.1. The Trimethylenemethane Dication (TMM²⁺). The resonance and inductive/field effects of the double bond on the double hydride abstraction enthalpy of **6** and **8** are obtained by extrapolation of those effects on their respective vinylogues (Figure 1a–c) to $n = 0$. Given the trends in Table 1, we can set a lower limit to those effects. It appears that the resonance effect in the Y-shaped species is at least 15.7 kcal/mol, and the magnitude of the inductive/field effect is at least 11.1 kcal/mol.

Extrapolation of the resonance effect in the Y-shaped vinylogues to $n = 0$ requires a model to describe the behavior of the resonance effect as a function of n . We chose to model the resonance effect using simple Hückel MO theory. Although simple Hückel theory has not proven to be reliable for absolute energies,^{43,44} it is reliable for *relative* energies in a homologous series. For example, in UV–vis spectroscopy, the λ_{\max} of linear conjugated polyalkenes, H₂C(CHCH)_{*n*}CH₂, tracks very well with that predicted by simple Hückel MO theory; the value of R^2 is greater than 0.99 for $n = 0–4$.

For each vinylogue of the dication in the parallel conformation, we calculated the relative total Hückel energy (in units of β) directly, taking into account all $4n + 2$ π -electrons delocalized over the entire molecule. For each vinylogue in the perpendicular conformation, we took the Hückel energy to be the sum of three independent π -systems: the isolated central double bond containing two electrons and the two conjugated chains, each with $2n$ electrons, on either side of the central double bond. The Hückel resonance contribution by the central double bond was taken to be the difference of those two energies. Relative values, in units of β , are listed in Table 1.

Our DFT-calculated resonance contributions of the Y-shaped vinylogues are plotted against the Hückel predicted resonance contributions in Figure 2. We note the good fit ($R^2 = 0.992$), which further provides support for the use of Hückel MO theory in our extrapolation.

Linear regression yields a slope of 96.55 and an intercept of -97.65 . In the trimethylenemethane dication ($n = 0$), the predicted Hückel resonance contribution is 1.464 β . Plugging in this value, we obtain a DFT resonance contribution of roughly 44 kcal/mol.

An orthogonal means by which to obtain the resonance contribution toward the double hydride abstraction enthalpy of the Y-shaped species is to extrapolate the inductive/field effects and then calculate by the difference. The difference between the double hydride abstraction enthalpy of **6** and that of **7** is taken to be the sum of the resonance and inductive/field effects. That difference is calculated at the DFT level to be 14.1 kcal/mol.

The inductive/field effect in the Y-shaped species is obtained by extrapolating the inductive/field effect in the Y-shaped vinylogues to $n = 0$. As with the extrapolation of the resonance effect, we need a function that describes the inductive/field effect as a function of n . We attempted two different fits, one assuming primarily inductive

(43) Schaad, L. J.; Hess, B. A. *J. Am. Chem. Soc.* **1972**, *94*, 3068.(44) Hess, B. A. J.; Schaad, L. J. *J. Am. Chem. Soc.* **1983**, *105*, 7500.

effects by the central double bond and one assuming primarily field effects.

Inductive effects are generally believed to fall off exponentially with distance.^{18,19,40,45} Therefore, modeling the inductive/field effects as purely inductive effects, we plotted the natural log of the magnitude of the inductive/field effect against n , the number of inserted vinyl units. However, the resulting correlation coefficient was not acceptable; the value of R^2 for these data was 0.98, whereas in our previous studies^{19,40} of singly charged species such a fit consistently yielded R^2 values of greater than 0.99. More importantly, the extrapolation to $n = 0$ did not agree well with the extrapolation of the resonance contribution to $n = 0$. That is, the sum of the extrapolated inductive/field effects and the extrapolated resonance effects was several kcal/mol different from the difference between the double hydride abstraction of the two parent compounds, **6** and **7**.

Modeling the inductive/field effects as purely field effects (i.e., charge repulsion), we plotted the inductive/field effects against $1/(n + 1)$. This was done because of the expected $1/r$ dependence of electrostatic interactions. This plot, shown in Figure 4, yields a straight line with a significantly higher correlation coefficient ($R^2 = 0.999$). Furthermore, this plot yields an extrapolated inductive/field effect that is in much better agreement with the extrapolated resonance effect. The best fit line of Figure 4 has a slope of -23.83 and an intercept of 0.86 . Plugging in $n = 0$ yields an inductive/field effect in the parent molecule of -23 kcal/mol. Subtracting this value from 14.1 kcal/mol (the difference in the double hydride abstraction enthalpies of **6** and **7**), we obtain a resonance energy of about 37 kcal/mol. This compares to 44 kcal/mol obtained from the direct extrapolation of the resonance effect to $n = 0$.

A.2. The Butadienyl Dication (BD^{2+}). An analogous treatment of the data is carried out for the resonance and inductive/field contributions toward the double hydride abstraction enthalpy of 2-butene (the linear system). We begin by setting a lower bound for both effects, given the increasing magnitude of each effect with decreasing n . The resonance effect in the $n = 1$ vinylogue of 2-butene is 7.8 kcal/mol, suggesting that the resonance contribution in the parent molecule is at least 7.8 kcal/mol. Similarly, the magnitude of the inductive effect in 2-butene is at least 15.9 kcal/mol.

As with the Y-shaped species, we employed Hückel MO theory as an aid to extrapolate the resonance effects in the linear species to $n = 0$. However, a slight modification was necessary because of a restriction on the delocalization of the π -electrons in the butadienyl dication and its vinylogues (we will discuss this later). To take that restriction into account, we assumed that the Hückel energy of each parallel vinylogue was better described by the completely conjugated linear system shortened by one carbon atom. The total Hückel energy of the butadienyl dication, for example, was taken to be the sum of the two electrons occupying the π_1 -orbital of the allyl system, with relative energy 1.414β . The total Hückel energy of the perpendicular conformation, on the other hand, was calculated just as before, and the Hückel

resonance contribution was computed as the difference in the two energies. Those values are listed in Table 2.

A plot of our DFT-calculated resonance contributions of the linear vinylogues against the Hückel resonance contribution is shown in Figure 3. There is an excellent fit ($R^2 = 0.9985$), once again suggesting that our use of Hückel theory is valid as a parameter with which to extrapolate the resonance contribution.

Linear regression yields a slope of 17.18 and an intercept of 0.87 . The predicted Hückel resonance contribution in BD^{2+} is 0.828β , which, upon plugging into the equation, yields a DFT resonance contribution of roughly 15 kcal/mol.

We also carried out an extrapolation of the inductive/field effect to $n = 0$ to obtain an independent measure of the resonance contribution. Similar to our extrapolations involving the Y-shaped vinylogues, we obtained an excellent fit (Figure 5) assuming a $1/(n + 1)$ dependence ($R^2 = 0.999$) of the inductive/field effect as opposed to an exponential decay ($R^2 = 0.985$). Linear regression assuming the $1/(n + 1)$ dependence yielded a slope of -35.50 and an intercept of 2.0 . Extrapolation to $n = 0$ gives rise to an inductive/field effect of about -34 kcal/mol.

The difference between the double hydride abstraction enthalpy of 2-butene and that of the reference molecule, butane, is -15.7 kcal/mol; that is, the double hydride abstraction enthalpy of 2-butene is 15.7 kcal/mol more endothermic than that of butane. If that difference is taken to be a sum of resonance and inductive/field effects brought about by the double bond in 2-butene, then subtraction of the extrapolated inductive/field effect should provide another measure of the resonance effect. Taking the extrapolated inductive/field effect to be -34 kcal/mol, we obtain a resonance effect of about 18 kcal/mol. This is in very good agreement with the 15 kcal/mol resonance contribution obtained from direct extrapolation of the resonance effect in the vinylogues.

B. Orbital Deletion Procedure (ODP) Methodology. As can be seen from Table 3, **1** is the most stable resonance structure that we calculated for TMM^{2+} and **4** is the most stable resonance structure that we calculated for BD^{2+} . **10** is less stable than **1** in part because of the additional charge repulsion among the terminal carbon atoms. It is further due to the fact that in **10** there is one fewer atom with an octet. Some stabilization is returned, however, by the favorable electrostatic interactions between the central negative charge and the three adjacent positive charges. **11** is less stable than **1** largely because of additional charge repulsion; in **11**, the central positive charge is adjacent to three partial positive charges, whereas in **1**, the positive charges are separated by two bonds. Similarly, **12** is less stable than **4** as a result of the adjacent positive charges.

Some assurance that we are indeed calculating the energies of electron-localized species is provided by the adiabatic geometries (Table 4). The fully delocalized TMM^{2+} species has three equivalent carbon-carbon bonds measuring 1.413 \AA , which is intermediate between a formal C-C single bond (about 1.54 \AA in ethane) and a formal C=C double bond (about 1.33 \AA in ethene). When the geometry of **1** is allowed to relax, the species that is generated possesses two distinct carbon-carbon bonds. One of those bonds is 1.342 \AA , which is shorter

(45) Bianchi, G.; Howarth, O. W.; Samuel, C. J.; Vlahov, G. *J. Chem. Soc., Perkin Trans. 2* **1995**, 7, 1427–1432.

than the bonds in the fully delocalized structure of TMM^{2+} . This bond resembles a formal C=C double bond, which measures about 1.33 Å in ethene. The other two carbon-carbon bonds are 1.491 Å, which is lengthened relative to the carbon-carbon bonds in TMM^{2+} . These $\text{C}(\text{sp}^2)\text{-C}(\text{sp}^2)$ single bonds resemble the C-C bond (1.54 Å) in ethane. The discrepancy comes from the electrostatic attraction between each positively charged terminal carbon and the double bond, which is also observed in the allyl cation³⁵ but not in linear polyenes.⁴⁶ In a similar fashion, relaxation of the geometry in **4** leads to a shortening of the C2-C3 bond and a lengthening of the C1-C2 and C3-C4 bonds. We note that these changes in bond length are less dramatic upon geometry relaxation.

We also note that the relative energies we calculate are quite insensitive to the basis set. All of the relative energies calculated using the different basis sets agree with one another to within about 5 kcal/mol and most are in agreement to within 1 or 2 kcal/mol.

The resonance energy of each dication is computed as the energy difference between the fully delocalized structure and the most stable resonance structure. If the geometry of the most stable resonance structure is taken to be that of the fully delocalized dication (i.e., the vertical geometry), then the vertical resonance energy (VRE) is computed to be about 56 kcal/mol using the 6-311+G(d,p) basis set. If the geometry of the most stable resonance structure is optimized, yielding the adiabatic geometry, then the adiabatic resonance energy (ARE) is computed to be about 48 kcal/mol using the 6-311+G(d,p) basis set. Similarly, the VRE of BD^{2+} is about 31 kcal/mol and the ARE is about 28 kcal/mol.

C. TMM^{2+} vs BD^{2+} . Our vinylogue methodology suggests that the resonance contribution to the double hydride abstraction enthalpy of **8** is about 15 kcal/mol. That of **6** is about 44 kcal/mol, suggesting that the resonance energy of TMM^{2+} is roughly 3 times that of BD^{2+} . Likewise, contribution by inductive/field effects toward the double hydride abstraction enthalpy of **8** is about -34 kcal/mol, whereas that of **6** is about -23 kcal/mol. This suggests that inductive/field effects serve to destabilize BD^{2+} more than TMM^{2+} by about 11 kcal/mol.

A very similar picture is provided by our ODP methodology, which suggests that the resonance energy of TMM^{2+} is substantially greater than that of BD^{2+} . The ARE of TMM^{2+} is about 48 kcal/mol, whereas the ARE of BD^{2+} is about 28 kcal/mol, which is nearly a difference of a factor of 2. Although the ODP methodology does not provide absolute contributions by inductive/field effects, it does provide the relative effects. Because the difference in resonance energy between TMM^{2+} and BD^{2+} is about 20 kcal/mol, which is about 4 kcal/mol greater than the difference in absolute energies of TMM^{2+} and BD^{2+} calculated at the HF/6-311+G(d,p) level, we can say that the inductive/field effects in BD^{2+} are about 4 kcal/mol more destabilizing than those in TMM^{2+} . This is in qualitative agreement with our vinylogue methodology, which suggests the same order but has a difference of about 11 kcal/mol.

The additional resonance energy in TMM^{2+} can be explained by simple resonance theory. Three classical

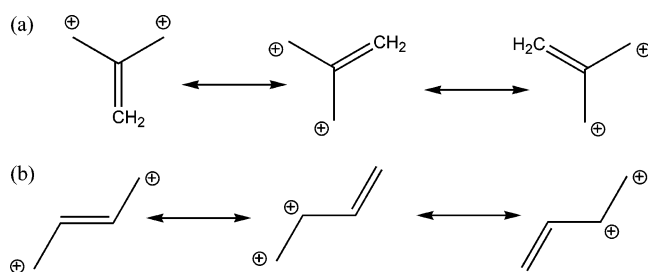


FIGURE 7. (a) Equivalent three classical resonance structures of TMM^{2+} . (b) Resonance structures of BD^{2+} . The two equivalent resonance structures are less stable than the unique one as a result of charge repulsion.

resonance structures can be drawn for both TMM^{2+} and BD^{2+} (Figure 7a). Those of TMM^{2+} are all equivalent such that each one contributes equally to the resonance hybrid thus maximizing the coupling among the three resonance structures.

For BD^{2+} , on the other hand, the three resonance structures are not all equivalent (Figure 7b). The resonance structure with the formal double bond on the central two atoms is clearly different from the other two structures. As shown in Table 4, the two equivalent resonance structures are poor contributors to the resonance hybrid, given the repulsion between adjacent positive charges. As a result, the delocalization of the π -electrons into the C1-C2 and C3-C4 bonding regions should be substantially inhibited. In other words, the two π -electrons of BD^{2+} are expected to be somewhat confined to the C2-C3 bonding region. This confinement of the electrons is likely what causes the resonance contribution of the linear system to be less than that of the Y-shaped system.

Natural bond orbital calculations^{47,48} at the HF/6-31+G* level of theory are in qualitative agreement with the conclusions from resonance theory. In both TMM^{2+} and BD^{2+} , the two π -electrons are distributed among a formal π molecular orbital between two carbon atoms and two atomic p-orbitals on the remaining two carbon atoms. The occupancy of the formal π -bond in TMM^{2+} is predicted to be 1.52 electrons, with the remaining 0.48 π -electrons being equally distributed in the atomic p-orbitals. In BD^{2+} , on the other hand, natural bond orbital calculations predict that 1.72 electrons occupy the formal π -bond between C2 and C3. The remaining 0.28 π -electrons reside in the atomic p-orbitals on C1 and C4. Natural bond orbital calculations, in summary, suggest that the two π -electrons in BD^{2+} are more localized in the π -bond than they are in TMM^{2+} .

As further evidence of the localization of the π -electrons in BD^{2+} , we note that there is little difference in the carbon-carbon bond lengths between the fully delocalized BD^{2+} and the adiabatic geometry of its most stable resonance structure, **4**. Even in the fully delocalized BD^{2+} species, the central carbon-carbon bond, measuring about 1.35 Å, strongly resembles a formal double bond. We compare this to the carbon-carbon bond length in

(46) Mo, Y. *J. Chem. Phys.* **2003**, *119*, 1300-1306.

(47) NBO 3.0: Glendening, E. D. R., A. E., Carpenter, J. E., Weinhold, F., Department of Chemistry, University of Wisconsin: Madison, WI.

(48) Foster, J. P.; Weinhold, F. *J. Am. Chem. Soc.* **1980**, *102*.

TMM²⁺, measuring about 1.41 Å, which resembles a bond that is more intermediate between a formal single bond and a formal double bond.

D. Dications vs Allyl Cations. Both the vinylogue methodology¹⁸ and the ODP methodology³⁵ were previously employed to determine the resonance energy of the allyl cation H₂C=CH-CH₂⁺, a monocation with two π-electrons delocalized over three carbon atoms. The vinylogue methodology yielded a resonance energy of about 20–22 kcal/mol, suggesting that inductive effects of the double bond account for about 5–7 kcal/mol of destabilization. The ODP methodology yielded a vertical resonance energy of about 45 kcal/mol and an adiabatic resonance energy of about 37 kcal/mol.

Using either methodology, we observe that the resonance energy of TMM²⁺ is greater than that of the allyl cation and that the resonance energy of BD²⁺ is less than that of the allyl cation. The vinylogue methodology suggests that the resonance energy of TMM²⁺ is roughly 20 kcal/mol greater than that of the allyl cation, and the ODP methodology suggests that the resonance energy is about 11 kcal/mol greater. The vinylogue methodology suggests that the resonance energy of BD²⁺ is about 5 kcal/mol less than that of the allyl cation, and the ODP methodology suggests that the resonance energy is about 9 kcal/mol less.

It is logical that the resonance energy of TMM²⁺ is greater than that of the allyl cation, given the additional conjugation in TMM²⁺ (4 atoms vs 3). In addition, resonance in TMM²⁺ leads to the delocalization of two positive charges, as opposed to only one in the allyl cation.

On the other hand, using these same arguments, it seems counterintuitive that the resonance energy of BD²⁺ is, in fact, smaller than that of the allyl cation. However, this is not surprising if we take into account arguments made earlier, which suggest that the π-electrons are substantially localized between C2 and C3 because of the strong electrostatic repulsion between the two formal positive charges. Our results here suggest that the π-electrons in BD²⁺ may even be more localized than the electrons in the allyl cation.

We can also compare the nonresonance effects we obtain for the allyl cation to those we obtain for TMM²⁺ and BD²⁺. In the allyl cation, those effects, brought about by the double bond, are expected to be primarily inductive effects. Internal charge repulsion within a specific resonance structure is expected to be significantly less than that in either TMM²⁺ or BD²⁺ because the species possesses only a single positive charge.

The inductive effects of the double bond in the allyl cation serve to destabilize the monocation by roughly 5 kcal/mol. In TMM²⁺ and BD²⁺, we would expect the inductive destabilization brought about by the double bond to be, at most, about 10 kcal/mol. We would certainly expect it to be higher with two positive charges instead of one, but we would expect it to be not quite double as a result of diminishing returns often seen with inductive effects. Therefore, only a fraction of the 23 and 34 kcal/mol destabilization observed in TMM²⁺ and BD²⁺, respectively, appears to be due to inductive effects. The bulk of that destabilization appears to be due to charge repulsion.

With the understanding that the destabilization in each dication is primarily due to charge repulsion,

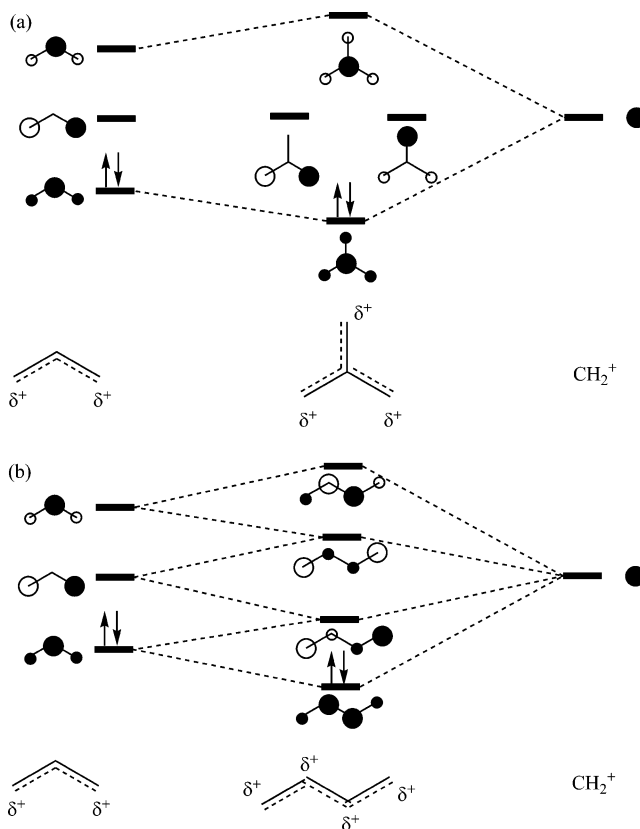


FIGURE 8. Hückel perturbation MO picture of (a) TMM²⁺ and (b) BD²⁺ as a union between the allyl cation (left) and a methylene cation (right). In forming TMM²⁺, the union is at the central carbon of the allyl cation, where the positive charge is not shared. In forming BD²⁺, the union is at the terminal carbon of the allyl cation, where there is significant positive charge.

perturbation Hückel MO theory (Figure 8) can account for the substantially greater destabilization in BD²⁺ over TMM²⁺. Both TMM²⁺ and BD²⁺ can be viewed as the union between a methylene cation and an allyl cation. To arrive at TMM²⁺, that union takes place at the central carbon of the allyl cation, where there is a node in the nonbonding π MO and, consequently, no charge. To arrive at BD²⁺, the union takes place at a terminal carbon of the allyl cation, where there is substantial contribution by the nonbonding MO and, consequently, significant positive charge. These results from perturbation MO theory are substantiated by the fact that in the plots of field/inductive effects vs 1/(n + 1) (Figures 4 and 5) the slope is of lesser magnitude for TMM²⁺ (slope = -23.83) than for BD²⁺ (slope = -35.50).

E. Evaluation of Y-Aromaticity. In general, the evaluation of aromaticity does not rely on energetic arguments alone. Other defining characteristics of aromaticity include the geometry of the species as well as its magnetic characteristics. Aromatic species have the tendency to be planar to allow for maximum overlap of the atomic p-orbitals on adjacent atoms. Additionally, aromaticity is readily seen in NMR spectra, particularly in the signals of aromatic protons and carbons.

TMM²⁺ is planar, which is consistent with an aromatic nature. Unfortunately, to our knowledge, no NMR studies have been conducted on TMM²⁺. However, the six-

electron system, TMM^{2-} , has been shown to exhibit NMR characteristics of an aromatic species.¹⁰

As mentioned in the Introduction, TMM^{2+} is more stable than its linear analogue, BD^{2+} , but the small difference in energy (about 9 kcal/mol) has cast doubt on its origin as being a special stability that we would call aromaticity. However, as we have argued throughout this paper, we cannot simply look at the 9 kcal/mol additional stability of TMM^{2+} over BD^{2+} because of the destabilization brought about by the inductive effects of the double bond and by the internal electrostatic repulsion in each dication. In contrast, when we evaluate the aromaticity of benzene by comparing, for example, the heat of hydrogenation of benzene to that of its acyclic analogue, 1,3,5-hexatriene, such inductive effects and electrostatic interactions are not at play. Instead, a comparison of those heats of hydrogenation essentially reflects just the difference in the resonance energies of the two systems. In a similar fashion, if we are to evaluate whether TMM^{2+} is aromatic on the basis of energetic arguments, then it is more sensible to make a direct comparison of each species' resonance energy, as we have done here.

Our methodologies suggest that the resonance energy of TMM^{2+} is worth about 40–50 kcal/mol and is roughly 2–3 times greater than that of its linear analogue, BD^{2+} . With this alone, it is tempting to conclude that TMM^{2+} exhibits aromatic stabilization. However, as we pointed out earlier, much of this difference in resonance energy appears to be a result of forced localization of the two π -electrons in BD^{2+} , originating from internal charge repulsion.

To put the resonance energies of TMM^{2+} and BD^{2+} in perspective, it may help to compare them to that of benzene, the prototype of aromaticity. Most studies place benzene's resonance energy between about 30 and 50 kcal/mol.^{49–56} These numbers are commensurate with those we obtained for TMM^{2+} , perhaps again suggesting that we may view the resonance stabilization of TMM^{2+} as aromatic in nature. However, we must be careful once again, given the different charges between TMM^{2+} and benzene. The resonance energy we calculated for TMM^{2+} is a convolution of at least two stabilizing phenomena, separate from aromaticity. One is electron delocalization via simple conjugation of the double bonds, which is analogous to the energy lowering of the quantum mechanical particle in a box when the box length is increased. The second stabilizing phenomenon is charge delocalization. In the delocalized TMM^{2+} species, the positive charge is less concentrated than in any of its resonance structures. The resonance energy of benzene, on the other hand, does not reflect charge delocalization because none of its resonance structures possess a formal charge.

(49) Cooper, D. L.; Geratt, J.; Ralmondt, M. *Nature* **1986**, *323*, 699–701.

(50) Shaik, S. S.; Hiberty, P. C.; Lefour, J. M.; Ohanessian, G. *J. Am. Chem. Soc.* **1987**, *109*, 363–374.

(51) Janoschek, R. *THEOCHEM* **1991**, *75*, 197–302.

(52) Matsunaga, N.; Cundari, T. R.; Schmidt, M. W.; Gordon, M. S. *Theor. Chim. Acta* **1992**, *83*, 57–68.

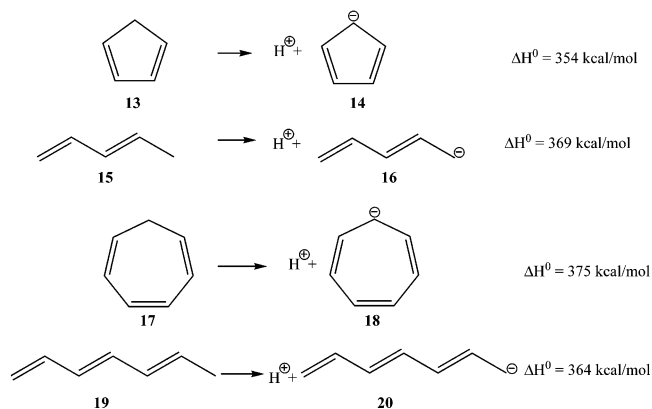
(53) van Lenthe, J. H.; Havenith, R. W. A.; Dijkstra, F.; Jenneskens, L. W. *Chem. Phys. Lett.* **2002**, *361*, 203–208.

(54) Mo, Y.; Wu, W.; Zhang, Q. *J. Phys. Chem.* **1994**, *98*, 10048–10053.

(55) Behrens, S.; Koester, A. M.; Jug, K. *J. Org. Chem.* **1994**, *59*, 2546–2551.

(56) Suresh, C. H.; Koga, N. *J. Org. Chem.* **2002**, *67*, 1965–1968.

In light of this, it may be beneficial to compare the difference in resonance energies between TMM^{2+} and BD^{2+} with differences in thermodynamic values involving aromatic, antiaromatic, and nonaromatic ions. We note that the gas-phase acidity⁵⁷ of cyclopentadiene (**13**), involving the aromatic cyclopentadienyl anion (**14**), is 354 kcal/mol, which is about 60 kcal/mol more exothermic than the acidities of linear alkanes. Much of the enhanced acidity of cyclopentadiene, however, appears to originate from phenomena other than what we can call aromaticity, i.e., charge delocalization as well as simple electron delocalization through conjugation. This conclusion comes from the fact that the acidity of 1,3-pentadiene (**15**), involving a nonaromatic anion (**16**) with the same number of π -electrons and a similar makeup, is 369 kcal/mol. We may conclude from this that the stabilization of the cyclopentadienyl anion brought about strictly by aromaticity, that is, over and above the stabilization brought about by simple conjugation and charge delocalization, is in the vicinity of 15 kcal/mol.



Similarly, we can examine the acidities of cycloheptatriene (**17**) and of 1,3,5-heptatriene (**19**). Deprotonation of the former yields an antiaromatic anion (**18**), whereas deprotonation of the latter yields a nonaromatic anion (**20**). The acidity of cycloheptatriene is 375 kcal/mol, whereas that of 1,3,5-heptatriene is 364 kcal/mol. It therefore appears that the destabilization brought about by the antiaromaticity within the cycloheptatrienyl anion is in the vicinity of 11 kcal/mol.

It is worth noting that the stability effects brought about by aromaticity and antiaromaticity within the cyclopentadienyl and the cycloheptatrienyl anions, respectively, are somewhat less than the difference in resonance energy we calculated for the TMM^{2+} and BD^{2+} , about 20–30 kcal/mol. It is therefore plausible that some of the additional resonance stabilization in TMM^{2+} can be attributed to the topology of electron delocalization or, in other words, “Y-aromaticity”.

Although it is quite clear that TMM^{2+} does exhibit substantial “extra” stability, it does not seem that its origin is the same as for that in species such as benzene. Benzene derives its extra stability from the cyclic nature of the contributing p atomic orbitals. The stability of TMM^{2+} , on the other hand, is critically dependent upon

(57) Bartmess, J. E. In *NIST Chemistry WebBook, NIST Standard Reference Database 69*; Mallard, W. G., Linstrom, P. J., Eds.; National Institute of Standards and Technology: Gaithersburg, MD, 1998.

the p-orbital on the central carbon atom, as evidenced by the fact that **11**, the resonance structure with the central p-orbital deactivated, is about 120 kcal/mol higher in energy than the fully delocalized optimal structure. In other words, the stability in TMM^{2+} does not originate from cyclic delocalization of the two π -electrons. Rather, it unambiguously originates from delocalization through the center.

F. Extrapolation Procedures in the Vinylogue Methodology. As was mentioned earlier, the extrapolation procedures of the resonance contributions were slightly different for the Y-shaped and linear vinylogues. For the Y-shaped vinylogues, we plotted (Figure 2) the DFT-calculated resonance contribution against the value obtained directly from Hückel MO theory. The result was a straight line with a positive slope.

For the linear vinylogues, on the other hand, that plot was not acceptable if the Hückel values of the actual vinylogues were used. Instead, a good fit was obtained upon using Hückel values for the completely conjugated linear species one carbon atom shorter than the actual vinylogues. The motivation for using these Hückel values stemmed from the apparent localization of the π -electrons in BD^{2+} between the central two carbon atoms as a result of internal charge repulsion. Hückel theory, however, does not take charge repulsion into account, such that it appears to overestimate π -electron delocalization in this case. We therefore artificially shortened the length over which the π -electrons were delocalized in the linear vinylogues by assuming a shorter carbon chain.

Overestimation of the π -electron delocalization in TMM^{2+} and its vinylogues, on the other hand, did not appear to be a problem. This may be indicative of the fact that there are no resonance structures of those species in which the two positive charges are on adjacent carbon atoms, as opposed to the linear dications.

The choice of a $1/(n + 1)$ dependence of the inductive effects also deserves discussion. Earlier, it was mentioned that it is perhaps the most logical to assume that the inductive effects fall off exponentially with distance between the substituent and the reaction center. This would directly fall out of a simplistic assumption that the distortion of electron density in a covalent bond, caused by the substituent, is proportional to the degree of electron deficiency of the substituent. In other words, the degree of electron deficiency of an atom adjacent to the substituent is some fraction of the degree of the electron deficiency of the substituent itself. In turn, the electron deficiency of the atom adjacent to the substituent causes an electron distortion in the covalent bond one more removed from the substituent. This defines an exponential decay with distance.

Bianchi⁴⁵ pointed out such an exponential decay of inductive effects in NMR studies. Furthermore, in our previous studies^{18,19,40} involving singly charged ions, both positive and negative, inductive effects were fit very well to exponential decays, with R^2 values of 0.99 or better.

The current study, however, involves dications, and we have argued that the nonresonance destabilization in each dication is primarily due to internal charge repul-

sion. We therefore believe that the $1/(n + 1)$ dependence of nonresonance destabilization is a reflection of the increase in internal charge repulsion as the conjugated chains in the vinylogues become shorter. This is because the $1/(n + 1)$ function follows the $1/r$ dependence expected by the repulsion between two charges.

Conclusions

Double hydride abstraction enthalpies were calculated for methylpropene (**6**) and 2-butene (**8**), along with their vinylogues in both their parallel and perpendicular conformations. Double hydride abstraction enthalpies were also calculated for reference molecules 2-methylpropane (**7**) and butane (**9**), along with their vinylogues. Differences in double hydride abstraction enthalpies among analogous (same n) parallel, perpendicular, and reference vinylogues yielded resonance and inductive/field effects in the vinylogues of **6** and **8**. Extrapolations of those values to $n = 0$ yielded resonance and inductive/field contributions toward the double hydride abstraction enthalpies of **6** and **8**. The resonance and inductive/field contributions involving **6** are about 44 and -23 kcal/mol, respectively. For **8**, those values are about 15 and -34 kcal/mol, respectively. These results suggest that the resonance stabilization of the trimethylenemethane dication (TMM^{2+}) is about 3 times that of the butadienyl dication (BD^{2+}).

An orbital deletion procedure (ODP) methodology was also performed on TMM^{2+} and BD^{2+} to obtain a direct measure of resonance energy in each dication. For TMM^{2+} , the vertical and adiabatic resonance energies were calculated to be about 56 and 48 kcal/mol, respectively. For BD^{2+} , those values were about 31 and 28 kcal/mol, respectively. The ODP methodology therefore suggests that the resonance energy of TMM^{2+} is roughly twice that of BD^{2+} .

Largely, we attribute this difference in resonance energies to localization of the π -electrons in BD^{2+} brought about by significantly more internal charge repulsion than in TMM^{2+} . On the basis of comparisons to resonance energies in other aromatic species, it is plausible that some of the difference in resonance energies between TMM^{2+} and BD^{2+} can be attributed to a special stabilization brought about by the topology of conjugation, i.e., Y-aromaticity.

Acknowledgment. We greatly appreciate the insightful comments provided by the referees, which helped to make this a much stronger paper. Funding was provided by a Cottrell College Science Award, No. CC5978, from Research Corporation. Support was also provided by the Elon University S.U.R.E. program.

Supporting Information Available: Cartesian coordinates and thermally corrected enthalpies of geometry-optimized species examined in the vinylogue methodology. Cartesian coordinates and energies of species examined in the ODP methodology. This material is available free of charge via the Internet at <http://pubs.acs.org>.

JO0508090